PCT WORLD INTELLECTUAL PROPERTY ORGANIZATION
International Bureau

INTERNATIONAL APPLICATION PUBLISHED UNDER THE PATENT COOPERATION TREATY (PCT)

(51) International Patent Classification 6 : A61B 5/00 — A1

(11) International Publication Number: **WO 99/43255**

(43) International Publication Date: 2 September 1999 (02.09.99)

(21) International Application Number: PCT/US99/04054

(22) International Filing Date: 25 February 1999 (25.02.99)

(30) Priority Data:
60/075,847 25 February 1998 (25.02.98) US

(71) Applicants *(for all designated States except US)*: UNIVERSITY OF IOWA RESEARCH FOUNDATION [US/US]; 106 Technology Innovation Center, Iowa City, IA 55242 (US). OHIO UNIVERSITY [US/US]; Ohio Univ. Innovation Center, One President Street, Athens, OH 45701 (US).

(72) Inventors; and
(75) Inventors/Applicants *(for US only)*: SMALL, Gary, W. [US/US]; 463 Adena Drive, The Plains, OH 45780 (US). BURMEISTER, Jason, J. [US/US]; 314 N. Governor Street, Iowa City, IA 52245 (US). ARNOLD, Mark, A. [US/US]; 445 N. 7th Avenue, Iowa City, IA 55242 (US).

(74) Agents: LARSON, Marina, T. et al.; Oppedahl & Larson LLP, P.O. Box 5270, Frisco, CO 80443-5270 (US).

(81) Designated States: AU, CA, JP, KR, US, European patent (AT, BE, CH, CY, DE, DK, ES, FI, FR, GB, GR, IE, IT, LU, MC, NL, PT, SE).

Published
With international search report.

(54) Title: NEAR INFRARED-TRANSMISSION SPECTROSCOPY OF TONGUE TISSUE

(57) Abstract

Non-invasive measurement of blood glucose levels is carried out using transmission spectroscopy on the tongue of the individual. The near infrared (NIR) first overtone spectral region between 7000 and 5000 cm^{-1} (1.43 – 2 μm) is well suited for non-invasive measurements. Because the tongue is one of the leanest accessible sights in the body, variations in readings due to body fat are minimal. Further, the tongue is well thermostated and vasculated which are important factors in selecting a measurement site.

FOR THE PURPOSES OF INFORMATION ONLY

Codes used to identify States party to the PCT on the front pages of pamphlets publishing international applications under the PCT.

AL	Albania	ES	Spain	LS	Lesotho	SI	Slovenia
AM	Armenia	FI	Finland	LT	Lithuania	SK	Slovakia
AT	Austria	FR	France	LU	Luxembourg	SN	Senegal
AU	Australia	GA	Gabon	LV	Latvia	SZ	Swaziland
AZ	Azerbaijan	GB	United Kingdom	MC	Monaco	TD	Chad
BA	Bosnia and Herzegovina	GE	Georgia	MD	Republic of Moldova	TG	Togo
BB	Barbados	GH	Ghana	MG	Madagascar	TJ	Tajikistan
BE	Belgium	GN	Guinea	MK	The former Yugoslav Republic of Macedonia	TM	Turkmenistan
BF	Burkina Faso	GR	Greece			TR	Turkey
BG	Bulgaria	HU	Hungary	ML	Mali	TT	Trinidad and Tobago
BJ	Benin	IE	Ireland	MN	Mongolia	UA	Ukraine
BR	Brazil	IL	Israel	MR	Mauritania	UG	Uganda
BY	Belarus	IS	Iceland	MW	Malawi	US	United States of America
CA	Canada	IT	Italy	MX	Mexico	UZ	Uzbekistan
CF	Central African Republic	JP	Japan	NE	Niger	VN	Viet Nam
CG	Congo	KE	Kenya	NL	Netherlands	YU	Yugoslavia
CH	Switzerland	KG	Kyrgyzstan	NO	Norway	ZW	Zimbabwe
CI	Côte d'Ivoire	KP	Democratic People's Republic of Korea	NZ	New Zealand		
CM	Cameroon			PL	Poland		
CN	China	KR	Republic of Korea	PT	Portugal		
CU	Cuba	KZ	Kazakstan	RO	Romania		
CZ	Czech Republic	LC	Saint Lucia	RU	Russian Federation		
DE	Germany	LI	Liechtenstein	SD	Sudan		
DK	Denmark	LK	Sri Lanka	SE	Sweden		
EE	Estonia	LR	Liberia	SG	Singapore		

NEAR INFRARED-TRANSMISSION SPECTROSCOPY OF TONGUE TISSUE

DESCRIPTION

Background of the Invention

This application relates to the non-invasive measurement and monitoring of chemical substances found in blood, and particularly to the non-invasive measurement and monitoring of blood glucose levels.

Diabetes affects approximately 16 million people in the United States. People suffering from diabetes mellitus must monitor their blood glucose levels for insulin replacement therapy. At present, this generally requires an invasive procedure, performed several times daily, in which a sample of blood is taken for analysis. Non-invasive procedures have been proposed, including those found in US Patents Nos. 5,069,229 and 5,459,317, and EP 0 548 418, which are incorporated herein by reference, but no in-home non-invasive glucose measurement device is as yet available.

Among the proposals for non-invasive measurement of blood chemicals are those which depend on diffuse-reflectance of infrared radiation, for example from a finger, lip or forearm. In these techniques, light is delivered to the surface of the tissue, penetrates for some distance and then is reflected back to be detected. The drawback of the diffuse reflectance measurements is that the depth to which the light penetrates is not deep enough to have enough interaction with glucose to provide consistent and quantitative detection of glucose. In addition, tissue areas conventionally used for diffuse reflectance measurements may have varying amounts of fat from individual to individual. Since fat interferes with detection of glucose, this variability can make calibration and quantification difficult.

It is an object of the present invention to provide an improved method for the non-invasive measurement of glucose.

Summary of The Invention

The present invention overcomes the difficulties of prior art processes by using transmission spectroscopy, and by performing the measurements on the tongue of the

individual. The near infra red (NIR) first overtone spectral region between 7000 and 5000 cm^{-1} (1.43 - 2 μm) is well suited for non-invasive measurements. Because the tongue is one of the leanest accessible sights in the body, variations in readings due to body fat are minimal. Further, the tongue is well thermostated and vasculated which are important factors in selecting a measurement site.

Brief Description of the Drawings

Fig. 1 shows SEP versus noise plots for model data sets. Vertical lines indicate noise levels of the webbing (solid) and tongue (dashed) for back to back spectra at different measurement wavelengths.

Figs. 2A-F show absorbance spectra for near-infrared measurements at different measurement sites.

Fig. 3 shows single beam spectra of human webbing (dashed) and tongue (solid) with a glucose absorbance spectrum (dotted) overlaid.

Figs. 4 A and B show 100% lines of back-to-back psectra of human webbing and tongue with an absorbance spectrum of 1M glucose overlaid.

Figs. 5A-E show glucose concentrations versus sample number for the calibration samples for five individuals.

Figs. 6 A-D show SEP versus RMA noise calculated over 100 cm^{-1} spectral ranges for model data sets. Circles and triangles are 5.6 and 6.3 mm aqueous thickness without scatter, respectively. Squares are prediction errors from the model data set with scattering particles added. The vertical lines are noise levels of subject D who had an aqueous layer thickness of 5.5 mm.

Figs. 7A-E are concentration correlation plots for the best PLS models for the five volunteers predicting the blind samples.

Figs. 8A-E are concentration plots for the five volunteers, using the first sample as the calibration and the last samples as the prediction.

Detailed Description of the Invention

In accordance with the present invention, non-invasive monitoring of glucose in a human patient, is carried out by measuring the near infrared absorbance of glucose using transmission spectroscopy on the tongue of the human patient. This selection of measurement site provides better correlation with invasive measurements than non-invasive measurements performed at other sites, including the index finger and webbing of the hand.

In selecting a site for non-invasive glucose determination, several factors need to be considered. First, a useful technique needs to produce results which are reliable predictors of the actual glucose levels. Second, it would be desirable to have a calibration model which would work in substantially all patients. Patient-to-patient variation in the physical size of the tissue being measured and in the levels of interferents such as fats, which can act as a major interferent in the measurement of glucose in the overtone region, can make achieving these goals a complicated process. Our evaluation of several alternative measurement sites, however, indicates that the tongue is a highly suitable location for non-invasive glucose measurements.

To evaluate various sites for their suitability, single beam transmission spectra were collected of human webbing between the thumb and forefinger, tongue, nasal septum, cheek, upper lip and lower lip. As described below, the hand webbing had the highest levels of fat in the individuals tested, thus producing the worst results, while the tongue had the lowest fat levels and produced the most accurate and reproducible results.

EXAMPLE 1

Evaluation of Alternative Measurement Sites

Spectra were collected on a modified Midac spectrometer for the near infrared range. Modification include laser detectors, a fan designed to control temperature in the spectrometer, a 250-Watt source operating at about 110 watts and a one-millimeter diameter InGaAs detector with a 1.9 μm cutoff (Epitaxx). An H-band astronomical filter was used to limit the source bandpass to utilize the full dynamic range of the detector without saturation and minimize sample heating. A one-inch diameter, 25 mm focal length convex lens was used to focus the source intensity on the sample or fiber optic bundle.

Preliminary single beam spectra were collected using a fiber optic bundle (*Dolan Jenner Industries*) connected to the thickness controlling window to direct the incident radiation to the sampling site. The detector and mount was freed from the spectrometer for ease of sampling. This arrangement allowed spectra to be collected from hard to reach body sites. Single beam transmission spectra were collected of human webbing between the thumb and forefinger, tongue, nasal septum, cheek, upper lip, and lower lip.

A background single beam spectrum was collected without a sample in the optical path using a combination of a neutral density filter to limit the incident source intensity and a low detector preamplifier gain setting to avoid detector and electronic saturation. The air spectrum was corrected to match the higher gain and incident radiation intensity of the tissue spectra before converting it to absorbance.

Spectra with lower noise levels were collected without the fiber optic bundle to maximize incident source intensity. The detector and mount were fixed in the spectrometer in a vertical position for the tongue spectra and in a horizontal position for the webbing spectra. A mirror was used to direct the incident radiation to the detector for the tongue spectra.

Absorption spectra of the webbing of 19 volunteers were collected. A regression analysis was performed to compute the thickness of water and fat from the spectra using beef fat and water as the standards. The average thickness of water was 4.67 mm and beef fat was 2.4 mm for a webbing thickness of 6 mm. Table 1 lists RMS noise levels for various frequency ranges of ten back-to-back webbing spectra of 128 scans each.

Figure 1 shows plots of SEP versus RMS noise levels for various frequency ranges for model spectra consisting of a constant fat thickness of 1.6 mm and variable water thicknesses of 5.6 and 6.2 mm. From Figure 1 and Table 1 , a very high SEP would be expected if the webbing were used (greater than 3 mM). The RMS noise levels are low in the spectral region which is dominated by water absorbance (>6000 cm^{-1}). The noise levels in the region dominated by fat absorbance are very high. They are an order of magnitude higher than the model spectra. Between measurement variations in the amount of fat compressed within the light path have not been successfully controlled. Another body site for the noninvasive measurement is needed because of the strong overlap between the absorbance bands of fat and glucose.

Table 1 RMS noise values calculated from webbing and tongue 100% lines.

Spectral Range (cm^{-1}) Sample	6400 -6300	6300 -6200	6200 -6100	6100 -6000	6000 -5900	5900 -5800
6 mm webbing	54.7	25.1	18.0	36.1	271.1	605.8
5.5 mm tongue	96.7	47.7	25.4	18.0	56.6	68.1

The composition and physical thickness of several bodily sites were evaluated with the goal of finding a suitable site for a noninvasive measurement of glucose. Absorption spectra are listed in Figures 2A through 2F. It is apparent from the spectra that the upper and lower lips, tongue, cheek and nasal septum have less fat than the webbing. A regression analysis was performed to quantify the amount of fat and aqueous thickness. Table 2 lists the calculated aqueous and fat thicknesses. The tongue was found to be most desirable because it has the least amount of fat and there are relatively few variations between people. Major disadvantages of the tongue are the possibility of spreading disease while sampling many people and the discomfort of collecting spectra.

Table 2 Calculated aqueous and fat thicknesses obtained from regression analysis.

Sample	Thickness (mm)	Aqueous thickness (mm)	Fat thickness (mm)	Scatter
Webbing	5.75	4.91	2.62	1.56
Upper lip	6	5.91	0.48	1.72
Lower lip	6	5.95	0.65	1.84
Tongue	6	5.61	0.26	1.47
Nasal septum	6	5.86	0.51	1.81
Cheek	6	5.61	0.37	1.61

Spectra were collected through the tongue of various people. The average thickness of fat and water was 0.2 and 5.9 mm, respectively, for the 10 volunteers who were sampled. Figure 3 shows single beam spectra of the human tongue and webbing collected under the same instrumental configuration with a superimposed absorbance spectrum of 1.0 M glucose. Although the spectrometer alignment was not held constant, the spectrum of the tongue is less absorbing and has less fat. Figure 4 shows 100% lines of back-to-back spectra of the human webbing and also from human tongue. Large variations in the fat bands which overlap with the glucose bands at 5920 and 5750 cm^{-1} in the webbing spectra makes it obvious that the tongue is a superior measurement site.

Table 1 also shows noise levels of tongue spectra calculated in the hospital with multiple interfaces. From these noise levels and Figure 2 one may estimate a SEP of about 2 mM on a one subject study.

It is clear that the tongue is a superior measurement site for a noninvasive measurement compared to the webbing. The convenience of collecting spectra through the webbing of the hand is traded for lower variations in the amount of fat within the light path. The interface between the spectrometer and the volunteer will need to be sterilized between collecting spectra from different subjects. If the same spectral quality were obtained in a noninvasive data collection as the test spectra from the tongue a SEP of about 2 could be obtained.

EXAMPLE 2

Detection of Blood Glucose Levels Using Transmission Spectroscopy of The Tongue

Spectra were collected over the course of 39 days on five type 1 diabetic volunteers, 3 female and 2 male. The experimental procedure was approved by a human subject protocol board at the University of Iowa Hospitals and Clinics. Two spectra and one reference blood glucose concentration were collected for each volunteer's visit which numbered greater than 100. The number of visits per day were limited to less than five per volunteer.

Spectra were collected using a Midac M-Series spectrometer modified for the NIR. The spectrometer modifications are detailed in Chapter 8. The source was held at 81.0 watts by supplying constant voltage. An H-band astronomical filter was used to limit the bandpass of the source intensity. The 1-mm diameter 1.9 μm cutoff InGaAs detector (Epitaxx) was held at 15 °C by supplying constant voltage to a thermal electric cooler. The resistor in the feedback loop of the first stage of the detector preamplifier was 27.1 kΩ. Interferograms (8K) were collected, Fourier transformed, and the resulting single beam spectra with a data spacing of 4 cm^{-1} were saved over the spectral range between 7000 and 5000 cm^{-1}. The temperature of the interface was held at 38.5 °C using a DC heating element and a temperature control circuit. The temperature was monitored at the following cites during the course of each data collection: room, interface, and inside the spectrometer.

Five interchangeable stainless steel interfaces were machined. These consisted of a cylindrical sheath to cover the detector and an adjustable lever which controls the sample thickness. Each piece had a hole machined through with a 11.5-mm diameter circular sapphire window to allow the source radiation to pass through the sample to be detected. The thickness of the sample was confined to 5.45 mm. The interchangeable interfaces were swabbed with 95% ethanol and autoclaved at 130 °C for 5 minutes between volunteer visits.

Reference Blood Glucose Values

Capillary blood from a finger stick was drawn into a 100 µL volume heparinized tube. These samples were analyzed immediately with a YSI 2300 Stat Plus glucose analyzer (Yellow Springs Instruments) with both probes measuring glucose. These reference values were validated with a simultaneous measurement using a One-touch test strip capillary blood glucose analyzer. The average of two YSI glucose values was used to build PLS models. Every fifth blood sample was considered a 'blind' and was not used to optimize the PLS models.

Data Analysis

Separate PLS models were optimized using single beam spectra from each individual. The first 189 spectra were not included because the source voltage varied and the volunteers were learning how to perform the measurement in this time period. Spectra were also removed if their single beam intensity was very low. A PCA score analysis was performed but no spectral outliers were removed. The PLS calibration

model parameters were optimized. Three unique rearrangements of calibration and monitoring sets were used to optimize spectral range and number of PLS factors. The parameters which gave the lowest average SEM for all three rearrangements of calibration and monitoring were selected. This procedure reduces the chance of over modeling and modeling information specific to a single small monitoring set .

Concentration Correlations

By limiting the number of samples that were collected each day, the correlation between glucose and time was minimized. Figure 5. shows plots of glucose versus sample number for the calibration samples for the five subjects. They look like scatter plots. Table 3 shows the correlation coefficient (r^2) of the time profiles. The correlation coefficients are all below 0.014. It is not likely that any temperature variation or spectrometer drift correlated with these randomized concentrations. In this way, spectral variations that the PLS models are built upon should only be analyte specific changes.

Table 3 Description of glucose concentrations.

subject	number	high (mM)	low (mM)	mean (mM)	standard deviation (mM)	Regression coefficents of time plots B_0	B_1	R^2
A	173	21.3	2.94	9.91	4.53	8.904	0.01082	0.01377
B	178	28.3	2.54	12.64	6.67	12.13	0.006442	2.465e-3
C	181	19.1	2.83	9.05	4.06	12.62	-2.203e-4	6.085e-6
D	207	26.85	3.20	11.88	5.09	8.625	5.032e-3	4.245e-3
E	169	16.75	3.79	8.57	2.83	8.793	-8.642e-4	2.020e-4

Significant glucose concentration variation is seen in all subjects except volunteer E who has very tight control over her glycemia. Table 3 lists the high, low, mean, and standard deviation of each subject's sample concentrations as well as the total number of spectra. The subjects were not persuaded to vary their daily diabetes treatments. The glucose concentrations are believed to be representative of the blood glucose variation for these individuals. Significant spectral and concentration changes are needed to build meaningful PLS calibration models. The limited concentration range for volunteer E might make calibration difficult.

Spectral Quality

The spectral quality is fairly high. Table 4 lists RMS noise levels calculated over 100 cm^{-1} intervals, the standard deviation of the ratio of the intensity at 5751 to 6994 cm^{-1}, standard deviation of the single beam intensity, and signal to noise ratio. The RMS noise levels were calculated using a second order polynomial fit for 100% lines from back-to-back single beam spectra. The noise levels between 6100 and 6000 cm^{-1} are fairly low but the noise levels between 6000 and 5900 cm^{-1} are not as low as those collected on the author in the pre-experiment trial. The ratio of the intensity at 5751 to 6994 cm^{-1} is the intensity at the fat band divided by the intensity at the peak of the single beam, respectively. The signal to noise (SNR) is the peak single beam intensity divided by the RMS noise of the single beam calculated between 7000 and 6800 cm^{-1}. The SD/mean intensity is the standard deviation of the peak single beam intensities divided by the mean peak intensity multiplied by 100%.

Comparison to Model

The *in vitro* model was used to estimate ideal prediction errors for the noninvasive data set. The aqueous layer thickness was estimated to be about 5.5 mm. By comparing the noninvasive noise levels to Figure 6 , it was estimated that an SEP of about 2.3 mM would be the best that could be expected for the noninvasive data if there were no interferences and no variation in the amount of fat in the optical path. The vertical lines are the noise levels from subject D. The SEP estimate for the 6000-5900 cm^{-1} plot is found by drawing a line between the models with and without scattering particles.

Table 4 Description of noninvasive spectral quality.

Subject	6100-6000 (μA.U.)	6000-5900 (μA.U.)	SD Intensity (5751/5994 cm^{-1})	SD/mean intensity(%)	SNR ($x10^4$)
A	26.9	95.1	0.007191	7.71	4.2
B	28.0	88.3	0.009485	8.08	3.5
C	26.6	89.8	0.005072	8.34	4.2
D	24.5	82.0	0.006365	9.64	3.9
E	31.1	99.1	0.011918	9.62	3.7

Predicting Blind Samples

The calibration data set was used to predict the blind samples using the optimal PLS parameters. Figure 7 A-E are concentration correlation plots for the best PLS models for the volunteers predicting the blind samples. The circled points are spectra in the blind that are not within the scatter of the calibration data. The circled point for volunteer D at about 11 mM was had the highest normalized intensity at 5943 cm^{-1} which is where protein absorbs. The circled point for volunteer C at 19 mM is the highest concentration sample in the data set. There seems to be a bias of under predicting high concentration samples. This bias was also observed in monitoring sets. The best SEP's are 2.70 and 2.66 for volunteers D and C with the high concentration samples removed, respectively.

Table 5 Optimal PLS parameters and prediction errors from predicting blind samples.

Who	Range (cm^{-1})	Factors	SEC (mM)	SEP_a (mM)	SEP_b (mM)	SDP (mM)
A	6510-5600	11	3.51	3.48		4.41
B	6310-5550	11	4.29	7.56*	5.50	6.75
C	6600-5650	11	3.04	3.49	2.66	3.73
D	6550-5620	16	2.52	3.96	2.70	4.69
E	6600-5650	10	2.62	3.35*		2.74

SEP_a includes all data in blind

SEP_b excludes circled data

* SEP is greater than SDC

In Figure 7B for subject B one point is not shown. The model predicted a blind sample at 48.9 mM when the actual concentration was 16.5 mM. The SEP without this point is 5.50 mM. The model for subject E is predicting the mean concentration. The slope is actually negative for this concentration correlation plot (Figure 7E). Even though the model has no prediction, 88% of the prediction points are in the A and B regions due to the limited concentration range of this subject. Table 6 lists the SEC, SEP, regression analysis and percentage of predicted samples in each of the regions on the Clarke error grid.

Table 6 Prediction errors and Clarke error grid analysis of predicting blind samples.

subject	SEC (mM)	SEP (mM)	SDP (mM)	Regression Analysis of Prediction Data			% of prediction in Clarke error grid Regions				
				B_0	B_1	R^2	A	B	C	D	E
A	3.51	3.48	4.41	4.031	0.5466	0.4333	54.1	37.8	8.1	0	0
B	4.29	7.56*	6.75	10.01	0.3393	0.1198	28.9	52.6	13.2	5.3	0
C	3.04	3.49	3.73	5.423	0.3710	0.2274	43.2	51.4	0	5.4	0
D	2.52	3.96	4.69	5.992	0.4543	0.3136	53.7	34.1	4.9	7.3	0
E	2.62	3.35*	2.74	8.778	-0.05689	0.01567	44.1	44.1	0	11.8	0

Predicting Last Part of Data

In a real world situation for in-home or clinical devices there will be an initial data collection used to build the calibration set. The model must be robust so it can accurately predict the concentrations of spectra following the initial calibration. Predicting the blind samples which were every fifth sample throughout the entire data collection is unrealistic in that there is a calibration sample before and after each blind sample. Spectrometer or temperature drifts could be more easily accounted for in this situation. To approximate a real world calibration, spectra from the beginning of the data collection were used as the calibration and spectra from the end of the data collection were predicted. The same PLS parameters used to predict the blind samples were used. Figures 8A through E are concentration correlation plots of the five volunteers using the first samples as the calibration and the last samples as the prediction. Table 7 shows details of the data sets and model performance.

Table 7 Prediction errors and Clarke error grid analysis of predicting last part of data.

subject	SEC	SEP	SDP	Regression Analysis of Prediction Data			% of prediction in Clarke error grid Regions				
	(mM)	(mM)	(mM)	B_0	B_1	R^2	A	B	C	D	E
A	3.27	4.42	4.72	7.562	0.2623	0.1643	26.9	55.8	5.8	11.5	0
B	4.77	6.08	6.58	10.69	0.2379	0.3129	17.6	52.9	20.6	2.9	5.9
C	2.96	3.86	4.11	8.027	0.3358	0.3067	40.7	50	5.6	1.9	1.9
D	2.73	3.35	5.44	4.119	0.6930	0.6303	54.2	35.4	2.1	10.4	0
E	2.71	2.72	2.66	8.577	0.06652	0.02379	43.8	56.2	0	0	0

In the noninvasive spectra there are two sources of RMS noise on 100% lines. The first is spectral noise from the detector and other electronic and optical components of the spectrometer. This noise is related to the number of photons at a given frequency which are detected by the detector. The *in vitro* model of a aqueous and fat layer of constant thickness produces this type of noise. The other type of noise is variation of strongly absorbing components such as fat and muscle. Although the noninvasive spectra have low noise in the spectral region dominated by water absorbance (greater than 6000 cm^{-1}), there are variations in the fat and muscle bands (below 6000 cm^{-1}) which are believed to be causing our high prediction errors. Subject E who had the worst PLS model had the highest variation in the fat band. This variation could be related to body composition or movement during the data collection.

The concentration correlation plot for subject E illustrates a situation where all predictions are in the A and B regions on the Clarke error grid but the model is clearly void of any analytical utility. This shows that the Clarke error grid alone is insufficient to judge analytical performance of PLS models.

Although, it is debatable whether glucose is being modeled for subjects A, B, and C. There is very strong evidence that glucose is being modeled for subject D. There is a bias of under predicting high concentration spectra. If this were due to a lack of analytical information the lower concentrations would be over predicted as with subject E. This is not the case. The predictions at low concentrations actually follow the unity line. It has been reported that there is a time delay in the increase of interstitial glucose concentration when blood glucose concentration is rising. When light passes through

the tongue it is believed that the majority of the photons will interact with interstitial fluid not blood. The mismatch between our predicted glucose values and reference blood glucose values at high concentrations accounts for scatter at high concentrations. There are conflicting claims in the literature about the exact relationship between blood and interstitial glucose concentrations. If the lower interstitial glucose does not track blood glucose at high concentrations, it would be further evidence that we are actually measuring glucose. This has never been observed before and is further evidence that we are measuring glucose absorbance information.

For the first time, a human noninvasive blood glucose measurement has been demonstrated. The calibration was such that glucose concentration was independent of sample order which eliminates the possibility of falsely low prediction errors due to chance correlations between glucose concentration and temperature or spectrometer drift. A real world calibration where data collected initially was used to predict data collected at a later time yielded similar prediction errors as predicting the blind samples which were every fifth sample throughout the data set.

For future measurements, an improved design for the interface may improve spectral reproducibility, thereby, reducing prediction errors. Also, the source power could be increased by at least 50% which would yield a higher signal to noise ratio. Although, spectral quality was probably compromised, the two-month data collection better approximates real world situations compared to calibrations over the course of one week.

CLAIMS

1. A method for non-invasive monitoring of glucose in a human patient, comprising measuring the near infrared absorbance of glucose using transmission spectroscopy, wherein the measurement is performed on the tongue of the human patient.

2. The method of claim 1, wherein the near infrared absrobance is measured in the first overtone spectral region between 7000 and 5000 cm^{-1}.

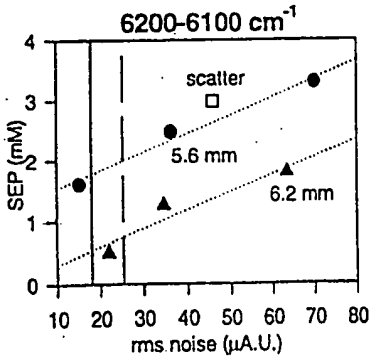

Fig. 1A

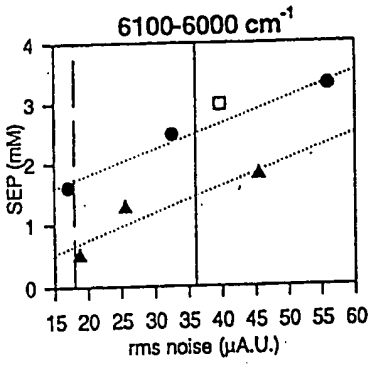

Fig. 1B

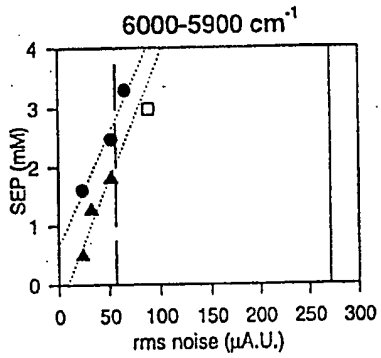

Fig. 1C

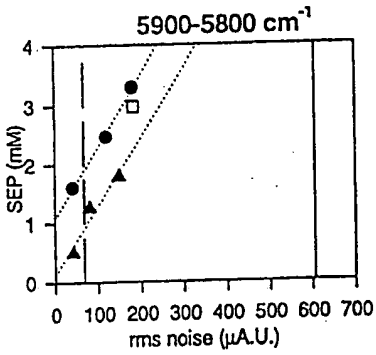

Fig. 1D

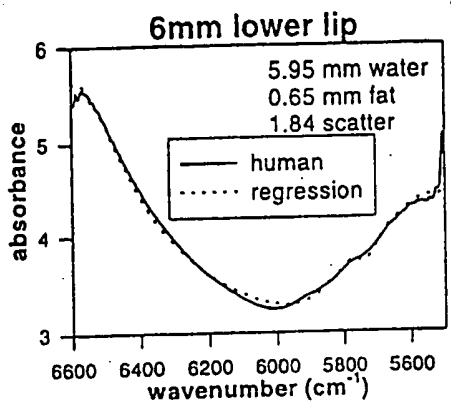

Fig. 2A

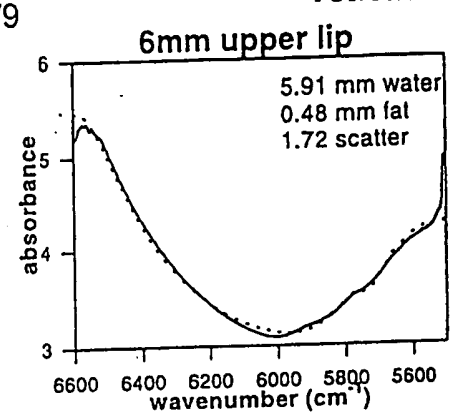

Fig. 2B

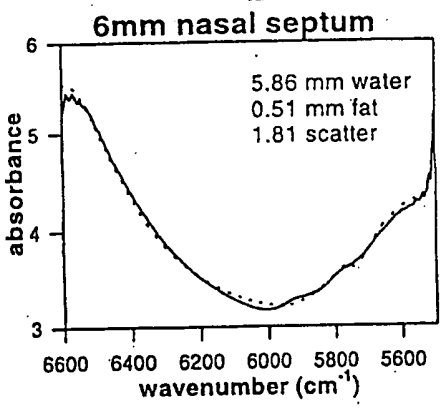

Fig. 2C

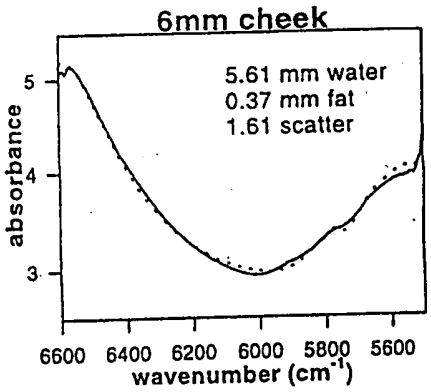

Fig. 2D

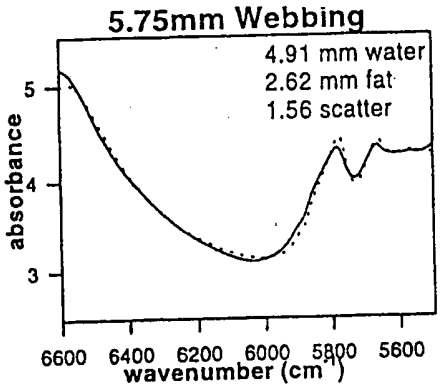

Fig. 2E

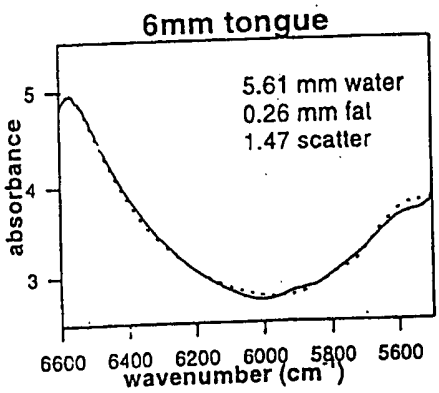

Fig. 2F

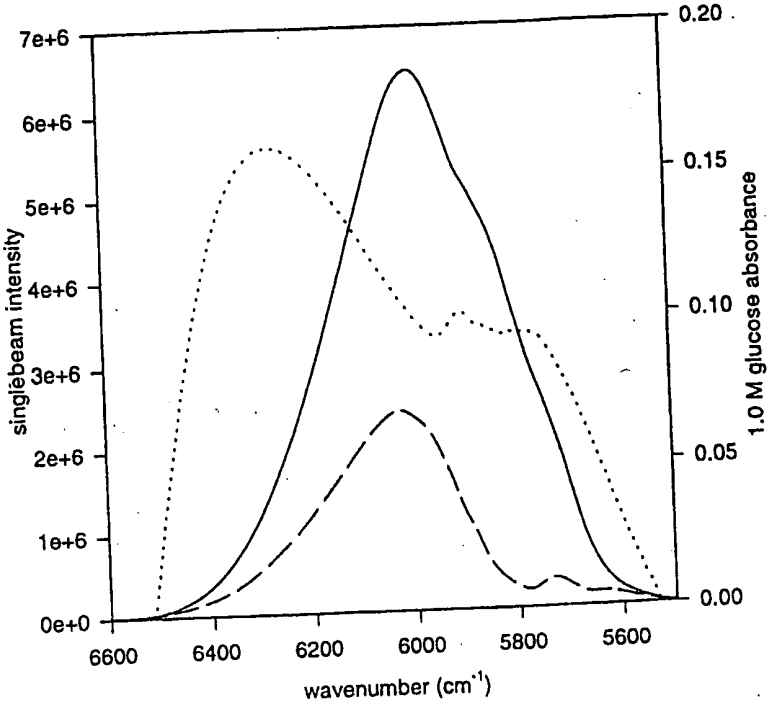
7e+6
6e+6
5e+6
4e+6
3e+6
2e+6
1e+6
0e+0
singlebeam intensity
0.20
0.15
0.10
0.05
0.00
1.0 M glucose absorbance
6600
6400
6200
6000
5800
5600
wavenumber (cm-1)

Fig. 3

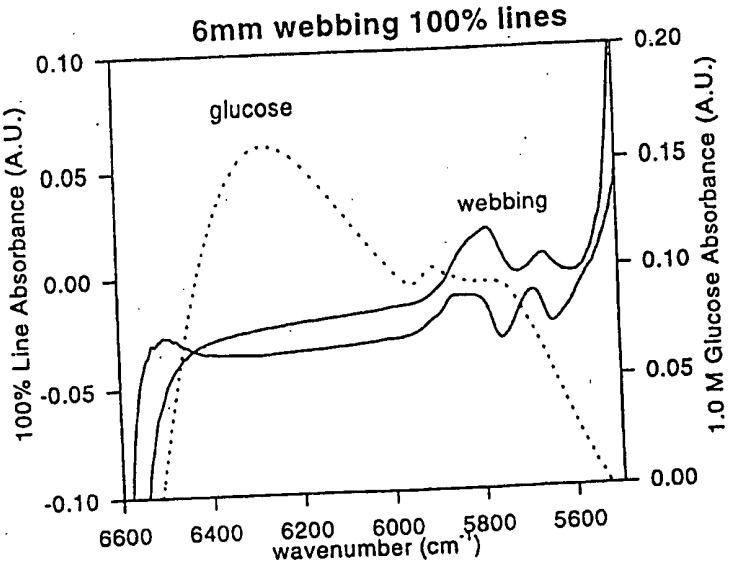
6mm webbing 100% lines
glucose
webbing
0.10
0.05
0.00
-0.05
-0.10
100% Line Absorbance (A.U.)
0.20
0.15
0.10
0.05
0.00
1.0 M Glucose Absorbance (A.U.)
6600
6400
6200
6000
5800
5600
wavenumber (cm-1)

Fig. 4A

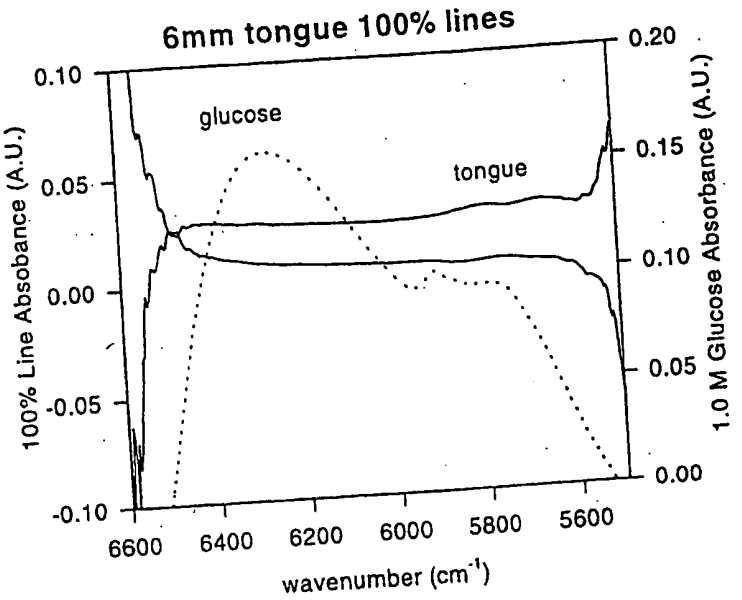

Fig. 4B

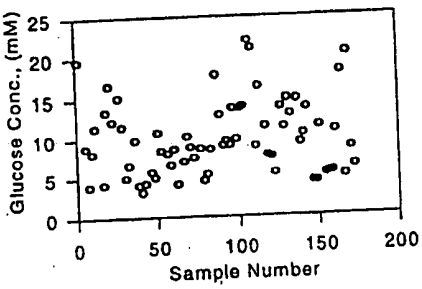

Fig. 5A

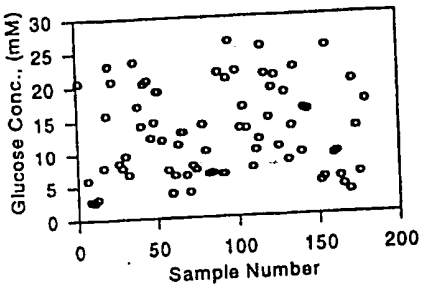

Fig. 5B

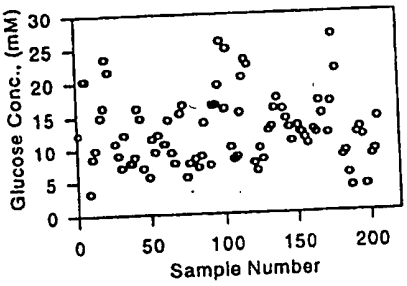

Fig. 5C

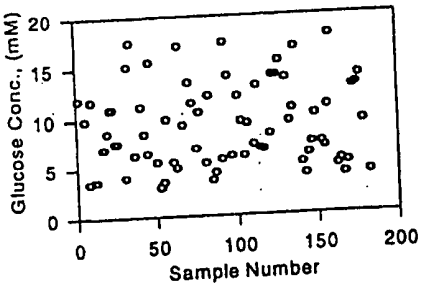

Fig. 5D

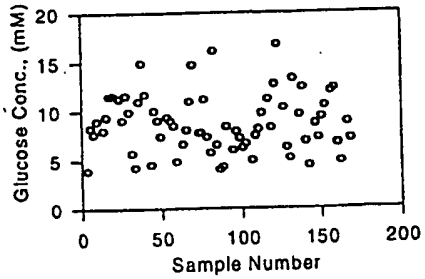

Fig. 5E

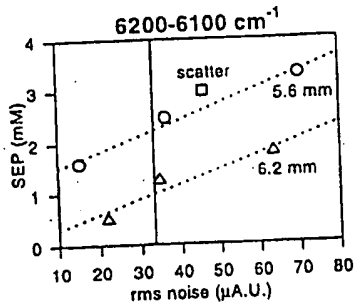

Fig. 6A

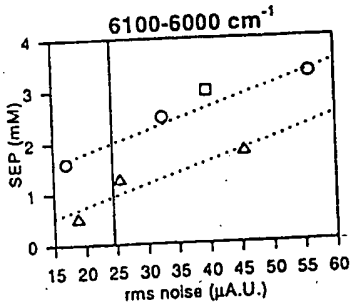

Fig. 6B

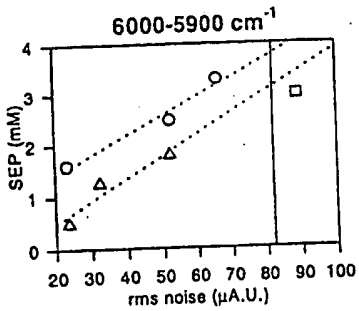

Fig. 6C

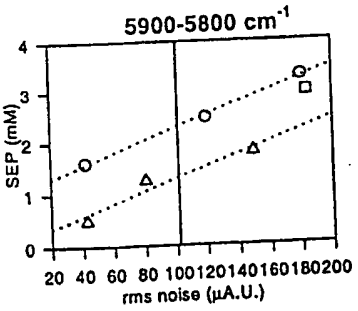

Fig. 6D

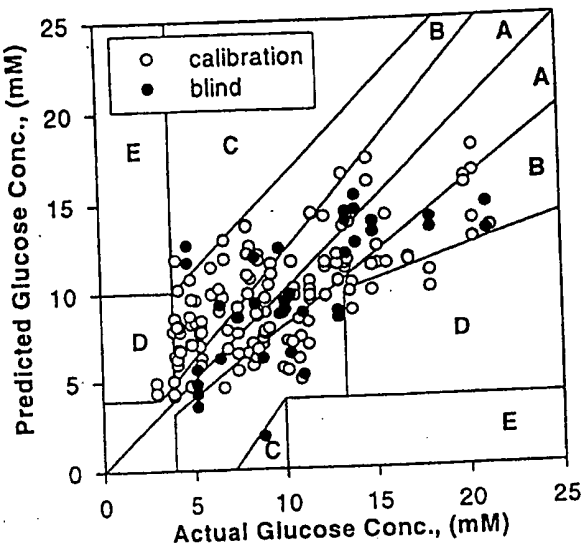
calibration
blind
A
A
B
B
C
C
D
D
E
E
Predicted Glucose Conc., (mM)
Actual Glucose Conc., (mM)
0
5
10
15
20
25

Fig. 7A

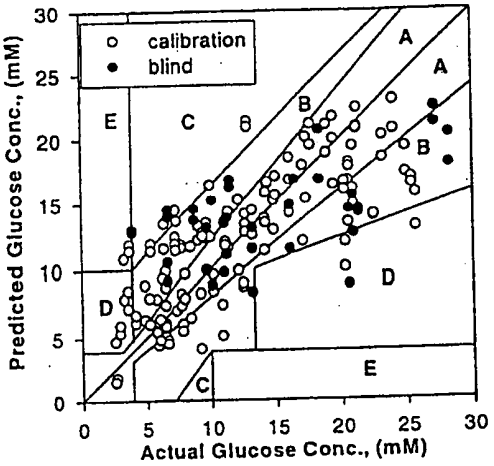
calibration
blind
A
A
B
B
C
C
D
D
E
E
Predicted Glucose Conc., (mM)
Actual Glucose Conc., (mM)
0
5
10
15
20
25
30

Fig. 7B

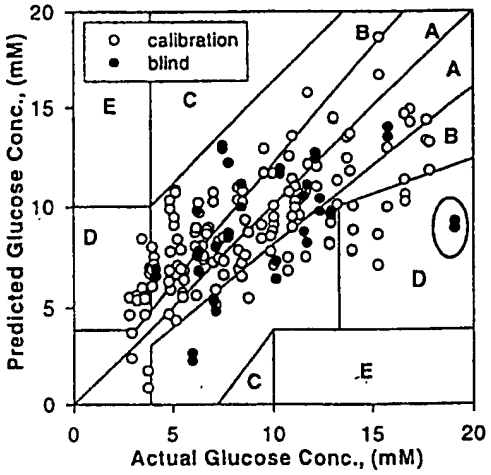

Fig. 7C

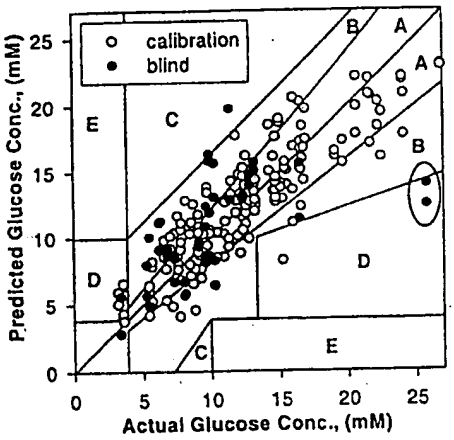

Fig. 7D

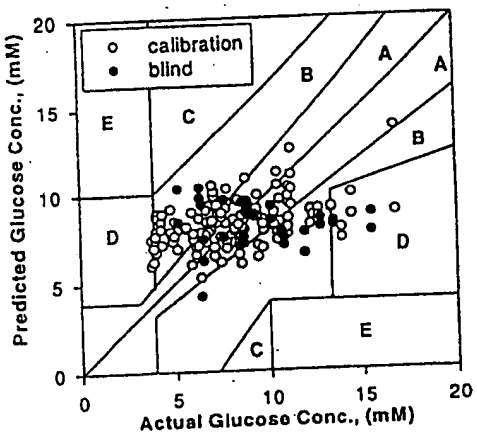

Fig. 7E

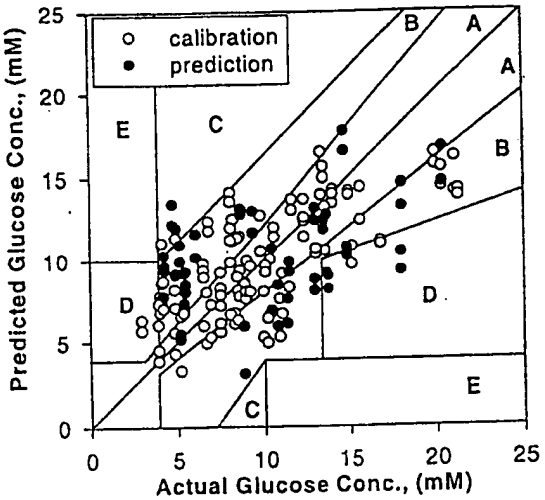
calibration
prediction
A
A
B
B
C
C
D
D
E
E
Predicted Glucose Conc., (mM)
Actual Glucose Conc., (mM)
0
5
10
15
20
25

Fig. 8A

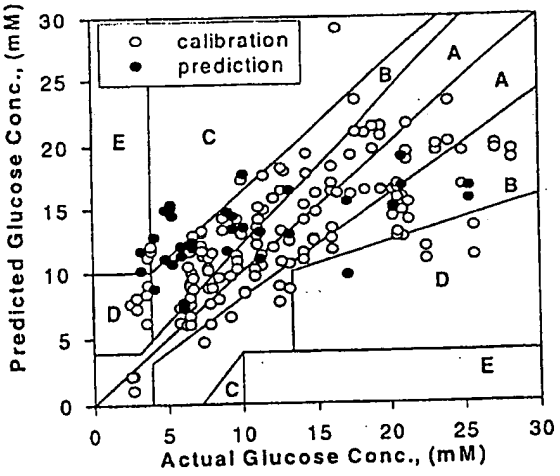
calibration
prediction
A
A
B
B
C
C
D
D
E
E
Predicted Glucose Conc., (mM)
Actual Glucose Conc., (mM)
0
5
10
15
20
25
30

Fig. 8B

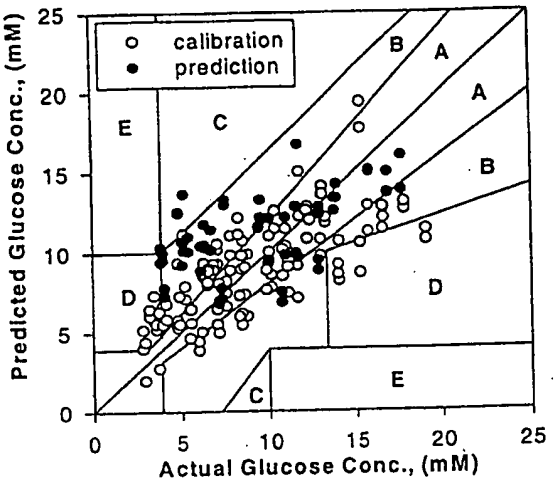

Fig. 8C

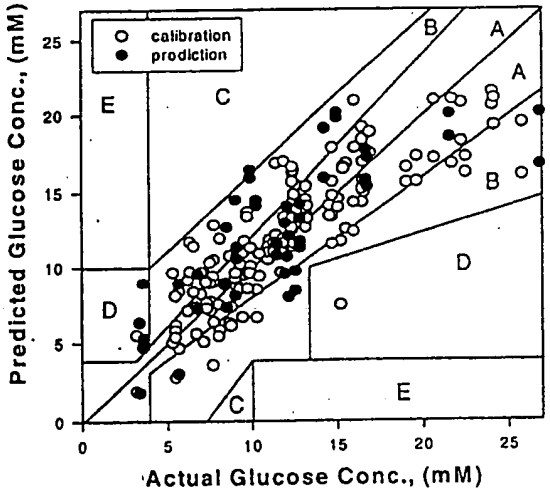

Fig. 8D

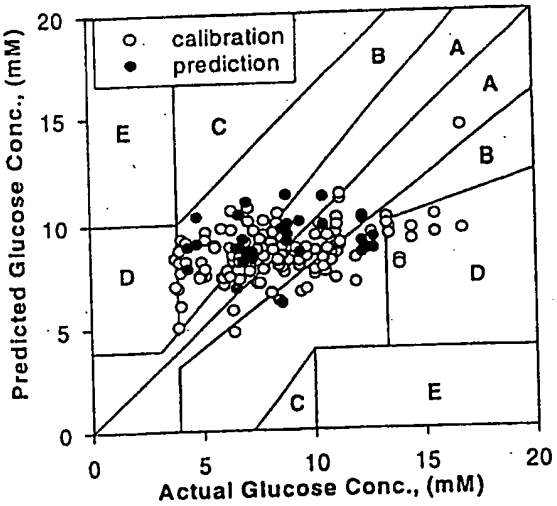

Fig. 8E

INTERNATIONAL SEARCH REPORT

International application No.
PCT/US99/04054

A. CLASSIFICATION OF SUBJECT MATTER

IPC(6) :A61B 5/00
US CL :600/316

According to International Patent Classification (IPC) or to both national classification and IPC

B. FIELDS SEARCHED

Minimum documentation searched (classification system followed by classification symbols)

U.S. : 600/310, 316, 322, 340

Documentation searched other than minimum documentation to the extent that such documents are included in the fields searched

Electronic data base consulted during the international search (name of data base and, where practicable, search terms used)

C. DOCUMENTS CONSIDERED TO BE RELEVANT

Category*	Citation of document, with indication, where appropriate, of the relevant passages	Relevant to claim No.
X	US 5,070,874 A (BARNES et al) 10 December 1991, col. 3 line 53.	1, 2
X	US 5,692,504 A (ESSENPREIS et al) 02 December 1997, col. 8 line 65 to col. 9 line 3.	1, 2

☐ Further documents are listed in the continuation of Box C. ☐ See patent family annex.

*	Special categories of cited documents:	"T"	later document published after the international filing date or priority date and not in conflict with the application but cited to understand the principle or theory underlying the invention
"A"	document defining the general state of the art which is not considered to be of particular relevance	"X"	document of particular relevance; the claimed invention cannot be considered novel or cannot be considered to involve an inventive step when the document is taken alone
"E"	earlier document published on or after the international filing date	"Y"	document of particular relevance; the claimed invention cannot be considered to involve an inventive step when the document is combined with one or more other such documents, such combination being obvious to a person skilled in the art
"L"	document which may throw doubts on priority claim(s) or which is cited to establish the publication date of another citation or other special reason (as specified)	"&"	document member of the same patent family
"O"	document referring to an oral disclosure, use, exhibition or other means		
"P"	document published prior to the international filing date but later than the priority date claimed		

Date of the actual completion of the international search 28 APRIL 1999	Date of mailing of the international search report 25 MAY 1999
Name and mailing address of the ISA/US Commissioner of Patents and Trademarks Box PCT Washington, D.C. 20231 Facsimile No. (703) 305-3230	Authorized officer ERIC F. WINAKUR Telephone No. (703) 308-3940

Form PCT/ISA/210 (second sheet)(July 1992)*